J|A|C|S ARTICLES

Published on Web 09/11/2009

Base-Promoted Ammonia Borane Hydrogen-Release

Daniel W. Himmelberger, Chang Won Yoon, Martin E. Bluhm, Patrick J. Carroll, and Larry G. Sneddon*

Department of Chemistry, University of Pennsylvania, Philadelphia, Pennsylvania 19104-6323

Received June 18, 2009; E-mail: lsneddon@sas.upenn.edu

Abstract: The strong non-nucleophilic base bis(dimethylamino)naphthalene (Proton Sponge, PS) has been found to promote the rate and extent of H_2-release from ammonia borane (AB) either in the solid state or in ionic-liquid and tetraglyme solutions. For example, AB reactions in 1-butyl-3-methylimidazolium chloride (bmimCl) containing 5.3 mol % PS released 2 equiv of H_2 in 171 min at 85 °C and only 9 min at 110 °C, whereas comparable reactions without PS required 316 min at 85 °C and 20 min at 110 °C. Ionic-liquid solvents proved more favorable than tetraglyme since they reduced the formation of undesirable products such as borazine. Solid-state and solution ^{11}B NMR studies of PS-promoted reactions in progress support a reaction pathway involving initial AB deprotonation to form the $H_3BNH_2^-$ anion. This anion can then initiate AB dehydropolymerization to form branched-chain polyaminoborane polymers. Subsequent chain-branching and dehydrogenation reactions lead ultimately to a cross-linked polyborazylene-type product. AB dehydrogenation by lithium and potassium triethylborohydride was found to produce the stabilized $Et_3BNH_2BH_3^-$ anion, with the crystallographically determined structure of the $[Et_3BNH_2BH_3]^-K^+$·18-crown-6 complex showing that, following AB nitrogen-deprotonation by the triethylborohydride, the Lewis-acidic triethylborane group coordinated at the nitrogen. Model studies of the reactions of $[Et_3BNH_2BH_3]^-Li^+$ with AB show evidence of chain-growth, providing additional support for a PS-promoted AB anionic dehydropolymerization H_2-release process.

Introduction

The development of a safe and efficient storage medium for hydrogen is vital to its use as an alternative energy carrier. One important approach to hydrogen storage has focused on the use of high-capacity chemical hydrides, including borohydrides, alanates, amineboranes, and metalloamidoboranes, as storage materials.[1,2] Understanding and controlling the many possible pathways by which dehydrogenation and regeneration of these materials can occur is key to their ultimate utilization and has therefore been a common goal of research efforts in chemical hydrogen storage.

Owing to its high hydrogen content, ammonia borane (AB) has been identified as one of the leading candidates for chemical hydrogen storage that could potentially release 19.6 wt % H_2 according to eq 1.[3]

$$H_3NBH_3 \rightarrow BN + 3H_2 \quad (1)$$

Utilization of waste heat from a proton exchange membrane fuel cell can provide for AB H_2-release reaction temperatures near 85 °C. However, at 85 °C in the absence of any additive, H_2-release from solid-state AB has been shown to exhibit an induction period of up to 3 h. After hydrogen release begins, only the release of ~1 equiv of H_2 can be achieved, rather than the 3 equiv predicted by eq 1, even with prolonged heating at 85 °C.[4,5] For AB to be useful for hydrogen storage, a fast and controlled H_2-release rate, as well as a viable AB regeneration method, must be achieved. A number of approaches have now been shown to induce AB H_2-release by a range of mechanistic pathways, including activation by transition metal catalysts,[6−21]

(1) Graetz, J. *Chem. Soc. Rev.* **2009**, *38*, 73–82.
(2) Hamilton, C. W.; Baker, R. T.; Staubitz, A.; Manners, I. *Chem. Soc. Rev.* **2009**, *38*, 279–293.
(3) Stephens, F. H.; Pons, V.; Baker, R. T. *Dalton Trans.* **2007**, *25*, 2613–2626.
(4) Stowe, A. C.; Shaw, W. J.; Linehan, J. C.; Schmid, B.; Autrey, T. *Phys. Chem. Chem. Phys.* **2007**, *9*, 1831–1836.
(5) Bluhm, M. E.; Bradley, M. G.; Butterick, R., III.; Kusari, U.; Sneddon, L. G. *J. Am. Chem. Soc.* **2006**, *128*, 7748–7749.
(6) Jaska, C. A.; Temple, K.; Lough, A. J.; Manners, I. *Chem. Commun.* **2001**, 962–963.
(7) Jaska, C. A.; Temple, K.; Lough, A. J.; Manners, I. *J. Am. Chem. Soc.* **2003**, *125*, 9424–9434.
(8) Jaska, C. A.; Manners, I. *J. Am. Chem. Soc.* **2004**, *126*, 2698–2699.
(9) Clark, T. J.; Lee, K.; Manners, I. *Chem.—Eur. J.* **2006**, *12*, 8634–8648.
(10) Clark, T. J.; Russell, C. A.; Manners, I. *J. Am. Chem. Soc.* **2006**, *128*, 9582–9583.
(11) Denney, M. C.; Pons, V.; Hebden, T. J.; Heinekey, D. M.; Goldberg, K. I. *J. Am. Chem. Soc.* **2006**, *128*, 12048–12049.
(12) Fulton, J. L.; Linehan, J. C.; Autrey, T.; Balasubramanian, M.; Chen, Y.; Szymczak, N. K. *J. Am. Chem. Soc.* **2007**, *129*, 11936–11949.
(13) Jiang, Y.; Berke, H. *Chem. Commun.* **2007**, 3571–3573.
(14) Keaton, R. J.; Blacquiere, J. M.; Baker, R. T. *J. Am. Chem. Soc.* **2007**, *129*, 1844–1845.
(15) Paul, A.; Musgrave, C. B. *Angew. Chem., Int. Ed.* **2007**, *46*, 8153–8156.
(16) Pun, D.; Lobkovsky, E.; Chirik, P. J. *Chem. Commun.* **2007**, 3297–3299.
(17) Blacquiere, N.; Diallo-Garcia, S.; Gorelsky, S. I.; Black, D. A.; Fagnou, K. *J. Am. Chem. Soc.* **2008**, *130*, 14034–14035.
(18) Douglas, T. M.; Chaplin, A. B.; Weller, A. S. *J. Am. Chem. Soc.* **2008**, *130*, 14432–14433.
(19) Staubitz, A.; Soto, A. P.; Manners, I. *Angew. Chem., Int. Ed.* **2008**, *47*, 6212–6215.
(20) Yang, X.; Hall, M. B. *J. Am. Chem. Soc.* **2008**, *130*, 1798–1799.

acid catalysts,[22] nano- and mesoporous scaffolds,[23−25] and ionic liquids.[5] There has likewise been significant recent progress in the development of efficient AB regeneration processes.[26]

We have previously shown[27,28] that the addition of small amounts of either LiH or $LiNH_2$ to AB in the solid state eliminated the induction period and increased both the rate and extent of H_2-release at 85 °C. As outlined in eqs 2 and 3, the initial step in these reactions was proposed to be AB deprotonation to produce the $H_3BNH_2^-$ anion, with this anion then inducing anionic dehydropolymerization of AB to produce a growing polyaminoborane polymer (eq 4).

$$H_3BNH_3 + Li^+NH_2^- \rightarrow H_3BNH_2^-Li^+ + NH_3 \quad (2)$$

$$H_3BNH_3 + Li^+H^- \rightarrow H_3BNH_2^-Li^+ + H_2 \quad (3)$$

$$H_3BNH_2^-Li^+ + H_3BNH_3 \rightarrow H_3BNH_2BH_2NH_2^-Li^+ + H_2 \quad (4)$$

Unfortunately, these reactions stopped after the release of ~1.5 equiv of H_2 due at least in part to the formation of the $LiBH_4$ side product via the reactions in eqs 5 and 6. Since $LiBH_4$ does not decompose until >350 °C, its formation reduces the extent of AB H_2-release at 85 °C.[29]

$$H_3BNH_2^-Li^+ \rightarrow (H_2BNH_2) + Li^+H^- \quad (5)$$

$$H_3BNH_3 + Li^+H^- \rightarrow Li^+BH_4^- + NH_3 \quad (6)$$

In order to avoid the formation of stable alkali-metal borohydrides, we investigated the use of alternative nitrogen-based deprotonating agents to induce AB polymerization. We report here that the strong (pK_a ~12), non-nucleophilic base bis(dimethyamino)naphthalene (Proton Sponge, PS)[30] can also induce AB H_2-release via an anionic dehydropolymerization mechanism with the advantage that the formation of a stable BH_4^- salt is avoided.

Experimental Section

Materials. All manipulations were carried out using standard high-vacuum or inert atmosphere techniques, as described by Shriver.[31] Ammonia borane (AB, Aviabor, 97% minimum purity) was ground into a free-flowing powder using a commercial coffee grinder. The 1-butyl-3-methylimidazolium chloride (bmimCl), 1,3-dimethylimidazolium methylsulfate (mmimMeSO$_4$), 1-butyl-2,3-dimethylimidazolium chloride (bdmimCl), and 1-ethyl-2,3-dimethylimidazolium ethylsulfate (edmimEtSO$_4$) ionic liquids (Fluka) were dried by toluene azeotropic distillation. Tetraethylene glycol dimethyl ether (tetraglyme, Sigma, 99%) and ethylene glycol dimethyl ether (glyme, Sigma, 99%) were vacuum distilled from sodium with heating. Bis(dimethylamino)naphthalene (Proton Sponge, PS, Aldrich) was sublimed and stored under inert atmosphere and light-free conditions. Lithium triethylborohydride (1.0 M solution in THF) and potassium triethylborohydride (1.0 M solution in THF) (Aldrich) were used as received.

Physical Measurements. The Toepler pump system used for hydrogen measurements was similar to that described by Shriver[31] and is diagrammed in the Supporting Information (Figure S1). The gases released from the reaction vessel were first passed through a liquid nitrogen trap before continuing on to the Toepler pump (700 mL). The released H_2 was then pumped into a series of calibrated volumes, with the final pressure of the collected H_2 gas measured (±0.5 mm) with the aid of a U-tube manometer. After the H_2-measurement was completed, the in-line liquid nitrogen trap was warmed to room temperature, and the amount of any volatiles that had been trapped was then also measured using the Toepler pump.

The automated gas buret was based on the design reported by Zheng et al.[32] but employed all glass connections, with a cold trap (−78 °C) inserted between the reaction flask and buret to allow trapping of any volatiles that might have been produced during the reaction.

Differential scanning calorimetry (DSC) was carried out on a Setaram C80 calorimeter. Samples containing 50 mg of AB and 50 mg of bmimCl, without and with 5 mol % (18 mg) of PS, were loaded into the cells under a N_2 atmosphere. The ramp rate was 1 °C/min, and samples were taken to either 85 or 110 °C.

While bmimCl is a liquid at 85 °C, it is a solid at room temperature; therefore, solid-state ^{11}B NMR analyses (at Pacific Northwest National Laboratories, 240 MHz machine spun at 10 kHz) were used to monitor the products of reactions carried out in bmimCl. All solid-state ^{11}B chemical shifts were measured relative to external $NaBH_4$ (−41 ppm). The solution ^{11}B NMR (128.4 MHz Bruker DMX-400 instrument) studies in the room-temperature ionic liquid mmimMeSO$_4$ were carried out by heating the reaction mixtures in sealed NMR tubes at 85 °C for the indicated times, with the spectra taken at 25 °C. The ^{11}B NMR spectra of the reactions in tetraglyme were collected with the NMR heated at 80 °C. All solid-state and solution ^{11}B NMR chemical shifts are referenced to external $BF_3 \cdot O(C_2H_5)_2$ (0.0 ppm), with a negative sign indicating an upfield shift.

Procedures for AB H_2-Release Reactions. For the experiments where the released H_2 was measured with the Toepler pump, the AB (250 mg, 8.1 mmol) was loaded into the reaction flasks under N_2. The solid-state reactions of AB/PS mixtures were carried out in evacuated 500 mL break-seal flasks that were heated in an oven preheated to the desired temperature. The solids were initially only crudely mixed, since upon heating the solid mixtures were found to form a melt before the onset of H_2-release. Reactions in solution were loaded into ~100 mL flasks with the ionic liquid and PS in the amounts given in the tables. The flasks were then evacuated, sealed, and placed in a hot oil bath preheated to the desired temperature. The flasks were opened at the indicated times, and the released hydrogen was quantified using the Toepler pump system. After reaction, the flasks were evacuated for 30 min through the cold trap to remove any volatile products from the reaction residue. The product residues and volatiles in the cold trap were extracted with dry glyme and analyzed by ^{11}B NMR.

For reactions using the automated gas buret, the AB (150 mg, 4.87 mmol) samples were loaded into ~100 mL flasks with

(21) Forster, T. D.; Tuononen, H. M.; Parvez, M.; Roesler, R. *J. Am. Chem. Soc.* **2009**, *131*, 6689–6691.
(22) Stephens, F. H.; Baker, R. T.; Matus, M. H.; Grant, D. J.; Dixon, D. A. *Angew. Chem., Int. Ed.* **2007**, *46*, 746–749.
(23) Gutowska, A.; Li, L.; Shin, Y.; Wang, C. M.; Li, X. S.; Linehan, J. C.; Smith, R. S.; Kay, B. D.; Schmid, B.; Shaw, W. J.; Gutowski, M.; Autrey, T. *Angew. Chem., Int. Ed.* **2005**, *44*, 3578–3582.
(24) Paolone, A.; Palumbo, O.; Rispoli, P.; Cantelli, R.; Autrey, T.; Karkamkar, A. *J. Phys. Chem. C* **2009**, *113*, 10319–10321.
(25) Sepehri, S.; Feaver, A.; Shaw, W. J.; Howard, C. J.; Zhang, Q.; Autrey, T.; Cao, G. *J. Phys. Chem. B* **2007**, *111*, 14285–14289.
(26) Davis, B. L.; Dixon, D. A.; Garner, E. B.; Gordon, J. C.; Matus, M. H.; Scott, B.; Stephens, F. H. *Angew. Chem., Int. Ed.* **2009**, *48*, 6812–6816.
(27) Sneddon, L. G. DOE Hydrogen Program Review, 2007; http://www.hydrogen.energy.gov/pdfs/review07/st_27_sneddon.pdf.
(28) Bluhm, M. E.; Bradley, M. G.; Sneddon, L. G. *Prepr. Symp.—Am. Chem. Soc., Div. Fuel Chem.* **2006**, *51*, 571–572.
(29) Fang, Z. Z.; Wang, P.; Rufford, T. E.; Kang, X. D.; Lu, G. Q.; Cheng, H. M. *Acta Mater.* **2008**, *56*, 6257–6263.
(30) Alder, R. W. *Chem. Rev.* **1989**, *89*, 1215–1223.
(31) Shriver, D. F.; Drezdzon, M. A. *Manipulation of Air Sensitive Compounds*, 2nd ed.; Wiley: New York, 1986.
(32) Zheng, F.; Rassat, S. D.; Helderandt, D. J.; Caldwell, D. D.; Aardahl, C. L.; Autrey, T.; Linehan, J. C.; Rappe, K. G. *Rev. Sci. Instrum.* **2008**, *79*, 084103-1–084103-5.
(33) (a) *CrystalClear*; Rigaku Corporation, 1999. (b) *Crystal Structure Analysis Package*; Rigaku Corp. Rigaku/MSC, 2002.

calibrated volumes, along with the ionic-liquid (150 mg) or tetraglyme (0.15 mL) solvents and PS. Under a flow of helium, the flask was attached to the buret system. The system was evacuated 30 min for reactions with the ionic-liquid solutions and 5 min for tetraglyme solutions. The system was then backfilled with helium and allowed to equilibrate to atmospheric pressure for ~30 min. Once the system pressure equalized, the data collection program was started, and the flask was immersed in the preheated oil bath. The data are reported from the point where the flask was initially plunged into the oil bath, but H_2-release was not observed until the ionic-liquid/AB mixture melted. Data were recorded at 2−5 s intervals, depending on the speed of the reaction. (Control experiments conducted without AB showed negligible pressure change, corresponding to <0.01 gas equivalent, when a helium-filled reaction flask connected to the gas buret was heated to 120 °C.) The product residues were extracted with dry glyme and analyzed by ^{11}B NMR.

Reactions of bmimCl and bmimCl/PS with partially dehydrogenated AB followed the procedures for the automated gas buret. Initially, two separate samples of neat AB (150 mg, 4.87 mmol) were heated for 23 h at 85 °C to release ~1 equiv of H_2. The reaction flasks were removed from the gas buret system under a flow of helium and then taken into a glovebox, where bmimCl (150 mg, 50 wt %) was added to one sample and bmimCl (150 mg, 50 wt %) and PS (55 mg, 5 mol %) were added to the second. After thorough mixing, the flasks were reattached to the gas buret system and heated again at 85 °C. Data were recorded on the gas buret system until H_2-release stopped.

Syntheses of $[Et_3BNH_2BH_3]^-M^+$ (M = Li and K). AB (50 mg, 1.6 mmol) was dissolved in THF or glyme (5.0 mL) and the solution cooled at −70 °C. Lithium triethylborohydride (1.0 M solution in THF, 1.6 mL) or potassium triethylborohydride (1.0 M solution in THF, 1.6 mL) was then added dropwise. After the solutions were warmed to room temperature and stirred for 1 h, their ^{11}B NMR spectra indicated the clean formation of $[Et_3BNH_2BH_3]^-M^+$ (M = Li or K). ^{11}B NMR (128.4 MHz, glyme, ppm): $[Et_3BNH_2BH_3]^-Li^+$ −7.5 (s, BEt_3) and −23.8 (q, BH_3); $[Et_3BNH_2BH_3]^-K^+$ −7.8 (s, Et_3B) and −23.6 (q, BH_3). DFT/GIAO calcd ^{11}B NMR chemical shift values for $Et_3BNH_2BH_3^-$: −10.6 (Et_3B) and −25.3 (BH_3). An electrospray mass spectrum of the $[Et_3BNH_2BH_3]^-Li^+$ solution confirmed the formation of the $Et_3BNH_2BH_3^-$ anion (calcd *m/e* for $^{12}C_6{}^1H_{20}{}^{11}B_2{}^{14}N$ 128, found 128).

Reactions of $[Et_3BNH_2BH_3]^-Li^+$ with AB. AB (50 mg, 1.6 mmol) was added to a glyme solution of $[Et_3BNH_2BH_3]^-Li^+$ (1.6 mmol, 5.0 mL) and then stirred at room temperature. After 18 h, the ^{11}B NMR spectrum (128.4 MHz, glyme, ppm) showed, in addition to the resonances from unreacted AB (−22.4) and $Et_3BNH_2BH_3^-$ (−7.5 and −23.8), new resonances at −6.0 (s, Et_3B), −10.9 (t, BH_2), and −19.6 (q, BH_3) that have chemical shift values consistent with the DFT/GIAO calculated values for the $Et_3BNH_2BH_2NH_2BH_3^-$ anion: −8.2 (Et_3B), −12.0 (BH_2), and −23.5 (BH_3). After 72 h, a Toepler pump measurement showed that 0.6 equiv of H_2 (relative to AB) had been released, and electrospray mass spectrometry confirmed the presence of both $Et_3BNH_2BH_3^-$ (*m/e* 128) and $Et_3BNH_2BH_2NH_2BH_3^-$ (calcd *m/e* for $^{12}C_6{}^1H_{24}{}^{11}B_3{}^{14}N_2$ 157, found 157).

The reaction rate increased when AB (0.1 g, 3.2 mmol) was reacted with a glyme solution (5.0 mL) of $[Et_3BNH_2BH_3]^-Li^+$ at 70 °C, and after only 2 h, electrospray mass spectrometry showed, in addition to $Et_3BNH_2BH_3^-$ (*m/e* 128) and $Et_3BNH_2BH_2NH_2BH_3^-$ (*m/e* 157), the formation of the higher oligomers $Et_3B(NH_2BH_2)_2NH_2BH_3^-$ (calcd *m/e* for $^{12}C_6{}^1H_{28}{}^{11}B_4{}^{14}N_3$ 186, found 186) and $Et_3B(NH_2BH_2)_3NH_2BH_3^-$ (calcd *m/e* for $^{12}C_6{}^1H_{32}{}^{11}B_5{}^{14}N_4$ 215, found 215).

(34) Altomare, A.; Burla, M.; Camalli, M.; Cascarano, G.; Giacovazzo, C.; Guagliardi, A.; Moliterni, A.; Polidori, G.; Spagna, R. *J. Appl. Crystallogr.* **1999**, *32*, 115–119.

Table 1. Summary of Structure Determination of $[Et_3BNH_2BH_3]^-K\cdot$18-crown-6

formula	$C_{18}B_2H_{44}NO_6K$
formula weight	431.26
crystal class	orthorhombic
space group	*Pbca* (no. 61)
Z	8
a, Å	11.5950(7)
b, Å	14.7764(9)
c, Å	29.239(2)
V, Å^3	5009.5(5)
μ, cm^{-1}	2.42
crystal size, mm	0.46 × 0.30 × 0.25
D_{calc}, g/cm^3	1.144
F(000)	1888
radiation	Mo Kα (λ = 0.71073 Å)
2θ range, deg	5.26−54.96
hkl collected	$-12 \le h \le 15$; $-19 \le k \le 14$; $-31 \le l \le 37$
temperature, K	143
no. reflections measured	20472
no. unique reflections	5721 (R_{int} = 0.0233)
no. observed reflections	4944 ($F > 4\sigma$)
no. reflections used in refinement	5721
no. parameters	430
R indices ($F > 4\sigma$)[a]	R_1 = 0.0374 wR_2 = 0.0892
R indices (all data)[a]	R_1 = 0.0459 wR_2 = 0.0943
GOF[b]	1.031
final difference peaks, e/Å^3	+0.240, −0.203

[a] $R_1 = \sum||F_o| - |F_c||/\sum|F_o|$; $wR_2 = \{\sum w(F_o^2 - F_c^2)^2/\sum w(F_o^2)^2\}^{1/2}$. [b] GOF = $\{\sum w(F_o^2 - F_c^2)^2/(n - p)\}^{1/2}$, where *n* is the number of reflections and *p* is the number of parameters refined.

Crystallographic Data for $[Et_3BNH_2BH_3]^-K^+\cdot$18-Crown-6. Single crystals of the $[Et_3BNH_2BH_3]^-K^+\cdot$18-crown-6 ($C_{12}H_{24}O_6$) adduct (Penn 3310) were grown from 1:1 mixtures of $[Et_3BNH_2BH_3]^-K^+$ and 18-crown-6 in THF/hexanes at room temperature.

Crystallographic data and structure refinement information are summarized in Table 1. X-ray intensity data were collected on a Rigaku Mercury CCD area detector employing graphite-monochromated Mo Kα radiation (λ = 0.71073 Å). Preliminary indexing was performed from a series of twelve 0.5° rotation images with exposures of 30 s. Rotation images were processed using CrystalClear,[33a] producing a listing of unaveraged F^2 and $\sigma(F^2)$ values which were then passed to the CrystalStructure[33b] program package for further processing and structure solution on a Dell Pentium III computer. The intensity data were corrected for Lorentz and polarization effects and for absorption.

The structure was solved by direct methods (SIR97).[34] Refinements were made by full-matrix least-squares based on F^2 using SHELXL-97.[35] All reflections were used during refinement (F^2 values that were experimentally negative were replaced by F^2 = 0). Non-hydrogen atoms were refined anisotropically, and hydrogen atoms were refined isotropically.

Computational Methods. DFT/GIAO/NMR calculations were performed using the Gaussian 03 program.[36] Geometries were fully optimized at the B3LYP/6-31G(d) level without symmetry constraints. The ^{11}B NMR chemical shifts were calculated at the B3LYP/6-311G(d) level using the GIAO option within Gaussian 03. The ^{11}B NMR GIAO chemical shifts are referenced to $BF_3\cdot OEt_2$ using an absolute shielding constant of 101.58, which was obtained

(35) Sheldrick, G. M. *SHELXL-97: Program for the Refinement of Crystal Structures*; University of Gottingen: Gottingen, Germany, 1997.
(36) Frisch, M. J.; et al. *Gaussian 03*, Revision B.05; Gaussian, Inc.: Pittsburgh, PA, 2003.

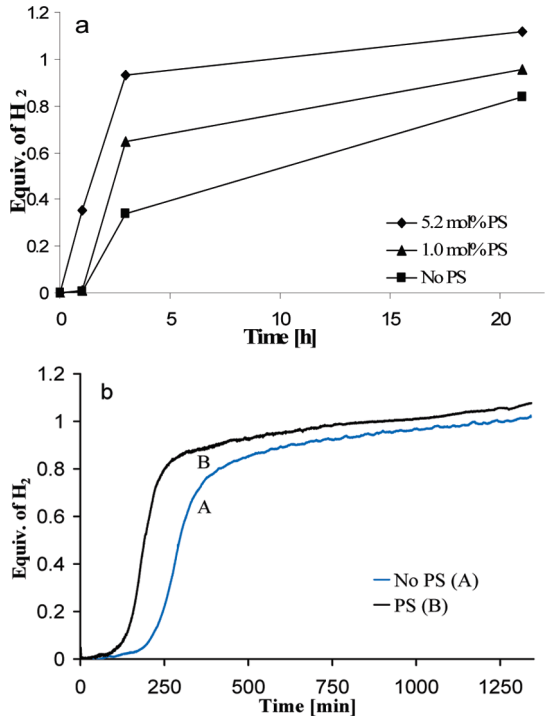

Figure 1. H_2-release measurements.(a) Toepler pump measurement for solid-state AB (250 mg) reactions with 0, 1.0, and 5.2 mol % PS (18 and 91 mg) at 85 °C. (b) Gas buret measurement for solid-state AB (150 mg) reactions with 0 and 5.2 mol % PS (55 mg) at 85 °C.

Table 2. H_2-Release Data (Toepler Pump) for AB/PS Solid-State Reactions at 85 °C

time (h)	amount of PS (mol %, mg, mmol)	total wt (mg)[a]	H_2 released	
			equiv	mmol
1		250	0	0
3		250	0.34	2.74
21		250	0.84	6.79
1	1.0, 18, 0.084	268	0	0
3	1.0, 18, 0.084	268	0.65	5.23
21	1.0, 18, 0.084	268	0.95	7.73
1	5.2, 91, 0.43	341	0.35	2.86
3	5.2, 91, 0.43	341	0.92	7.52
21	5.2, 91, 0.43	341	1.12	9.04

[a] 250 mg of NH_3BH_3 (8.1 mmol) was used for all reactions.

from the GIAO NMR calculated shift of $BF_3 \cdot OEt_2$ at the B3LYP/6-311G(d)//B3LYP/6-31G(d) level of theory.

Results and Discussion

H_2-Release from AB/PS Solid-State Reactions. As shown in Figure 1a and Table 2, initial H_2-release measurements using the Toepler pump of the solid-state reactions of AB in the presence of 1.0 and 5.2 mol % PS at 85 °C clearly demonstrated the activating effect of PS on AB H_2-release. While the reaction with 1.0 mol % PS still showed an induction period with no H_2 released after 1 h, the extent of release was significantly increased at 3 h (0.65 equiv) compared to that from pure AB at the same time (0.34 equiv). The data for the 5.2 mol % PS reaction indicated both a shortened induction period, with 0.35 equiv already released at 1 h, and significantly increased amounts of H_2-release at both 3 h (0.93 equiv) and 20 h (1.12 equiv) compared to those of either the pure AB or 1.0 mol % PS reactions. However, the solid-state AB/PS reactions stopped just after the release of ~1.1 equiv of H_2. More detailed H_2-release data collected (Table 3 and Figure 1b) for the 5.2 mol % PS reaction with the automated gas buret again clearly demonstrated that the induction period was shortened and the rate of H_2-release was increased upon the addition of 5.2 mol % PS.

Table 3. H_2-Release Data (Gas Buret) for AB/PS Solid-State Reactions at 85 °C

amount of PS (mol %, mg, mmol)	total wt (mg)[a]	time to H_2-equivalents (min)		
		0.5 equiv	1 equiv	final (equiv)
	150	295	1264	1333 (1.02)
5.3, 55, 0.26	205	191	885	1334 (1.08)

[a] 150 mg of NH_3BH_3 (4.87 mmol) was used for all reactions.

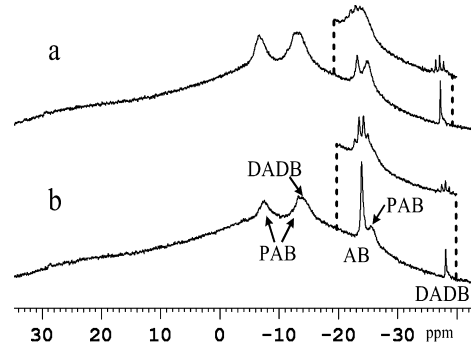

Figure 2. $^{11}B\{^1H\}$ NMR (128.4 MHz) spectra (insets show ^1H coupled spectra) recorded at 25 °C of the glyme extract of the reaction of (a) AB (150 mg) and 5.3 mol % PS (55 mg) at 85 °C for 22 h and (b) AB (150 mg) at 85 °C for 22 h. The broad DADB resonance at −13 ppm is obscured by the PAB resonance.

The NMR spectra in Figure 2 of the glyme-soluble residues from the solid-state AB/PS reactions showed features similar to those of the pure AB reactions. Thus, as the reaction progressed, the AB resonance (−23.5 ppm) decreased and was replaced by resonances arising from both the diammoniate of diborane, $[(NH_3)_2BH_2]^+BH_4^-$, (DADB; −13.3 (overlapped) and −37.6 ppm)[37,38] and branched-chain polyaminoborane polymers (PAB; −7, −13.3, and −25.1 ppm).[5] Consistent with the faster H_2-release found for the PS/AB mixtures, the spectra show that after 22 h the amount of unreacted AB was less in the PS/AB reactions than in the pure AB reaction. The solid-state ^{11}B NMR spectra in Figure 3 of the final products of the reactions showed an additional broad resonance centered near ~23 ppm that is characteristic of the sp^2 boron framework of cross-linked polyborazylene structures,[39−41] thus indicating that AB dehydrogenation ultimately produces B═N unsaturated products. Consistent with this conclusion, the ^{11}B NMR spectra of the volatile products of the PS/AB reactions collected in the cold trap through which the released H_2 had been passed also indicated some borazine ($B_3N_3H_6$) formation, with the amount of the volatiles (ranging from 0.04 to 0.25 mmol, depending upon the particular experiment) corresponding to <10% of the AB converting to borazine.

H_2-Release from AB/PS Solution Reactions. We have previously shown that polar solvents, especially ionic liquids such

(37) Onak, T. P.; Shapiro, I. *J. Chem. Phys.* **1960**, *32*, 952.
(38) Shore, S. G.; Parry, R. W. *J. Am. Chem. Soc.* **1958**, *80*, 20–24, and preceeding papers in the issue.
(39) Fazen, P. J.; Beck, J. S.; Lynch, A. T.; Remsen, E. E.; Sneddon, L. G. *Chem. Mater.* **1990**, *2*, 96–97.
(40) Fazen, P. J.; Remsen, E. E.; Beck, J. S.; Carroll, P. J.; McGhie, A. R.; Sneddon, L. G. *Chem. Mater.* **1995**, *7*, 1942–1956.
(41) Gervais, C.; Framery, E.; Duriez, C.; Maquet, J.; Vaultier, M.; Babonneau, F. *J. Eur. Ceram. Soc.* **2005**, *25*, 129–135.

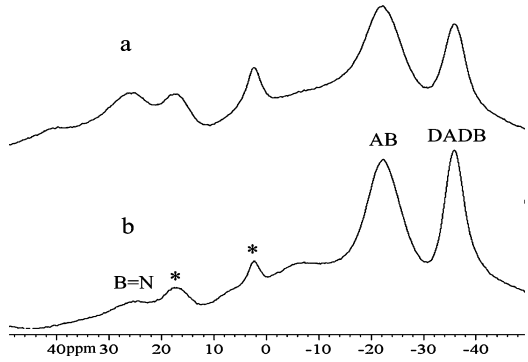

Figure 3. Solid-state ^{11}B NMR (240 MHz) spectra recorded at 25 °C of the reaction of (a) AB (150 mg) and 5.3 mol % PS (55 mg) at 85 °C until 1 equiv of H_2 was released and (b) AB (150 mg) at 85 °C until 1 equiv of H_2 was released. The broad DADB resonance at −13 ppm is obscured by the AB resonance. Borate resonances at 17 and 2 ppm result from exposure of the sample to air.

Table 4. H_2-Release Data (Toepler Pump) for AB/bmimCl/PS Reactions at 85 °C

time (h)	amount of PS (mol %, mg, mmol)	total[a] wt (mg)	H_2 released equiv	H_2 released mmol
1		500	0.69	5.62
3		500	1.00	8.10
6		500	1.28	10.36
23		500	1.97	15.94
1	0.5, 9, 0.04	509	0.83	6.70
3	0.5, 9, 0.04	509	1.65	13.37
6	0.5, 9, 0.04	509	2.10	17.04
22	0.5, 9, 0.04	509	2.23	18.04
1	5.2, 91, 0.43	591	1.40	11.33
3	5.2, 91, 0.43	591	2.10	17.02
6	5.2, 91, 0.43	591	2.18	17.67
21	5.2, 91, 0.43	591	2.23	18.04
1	24.9, 434, 2.03	934	0.79	6.37
3	24.9, 434, 2.03	934	1.75	14.14
6	24.9, 434, 2.03	934	2.01	16.28
22	24.9, 434, 2.03	934	2.13	17.23

[a] 250 mg of NH_3BH_3 (8.1 mmol) and 250 mg of bmimCl were used for all reactions.

as 1-butyl-3-methylimidazolium chloride (bmimCl), can activate H_2-release from AB at 85 °C,[5] with over 2 equiv being produced in ~5 h from a 50/50 wt % AB/bmimCl mixture. Comparisons of the H_2-release rates using Toepler pump measurements of AB dissolved in bmimCl with different amounts of added PS at 85 °C are summarized in Table 4 and Figure 4. In the absence of PS, only 0.69, 1.00, 1.28, and 1.97 equiv of H_2-equiv were released at 1, 3, 6, and 23 h, respectively. In contrast, a similar reaction of AB in bmimCl containing 5.2 mol % PS showed a significantly increased H_2-release rate, with 1.40 equiv of H_2-equiv released by 1 h and 2.10 equiv of H_2 released after only 3 h. Even when the amount of PS was decreased to only 0.5 mol % PS, there were still significant increases in the H_2-release found at 1 h (0.83 equiv), 3 h (1.65 equiv), and 6 h (2.10 equiv) compared to those of the reaction without PS. The plots in Figure 4 show that the biggest differences in the H_2-release rates of the bmimCl reactions with and without PS occurred following the release of the first equivalent of H_2. For the reaction without PS, the first equivalent was released in 3 h, and even after 23 h only 1.97 equiv was released. On the other hand, by 3 h the reactions with 5.2 and 1.0 mol % PS had already released 2.10

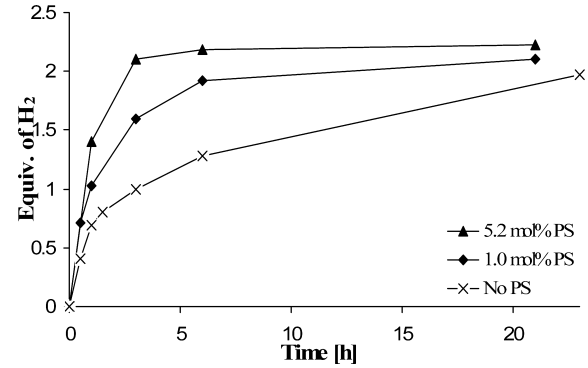

Figure 4. H_2-release measurements (Toepler pump) of the reaction of AB (250 mg) in bmimCl (250 mg) with 0, 1.0, and 5.2 mol % PS (18 and 91 mg) at 85 °C.

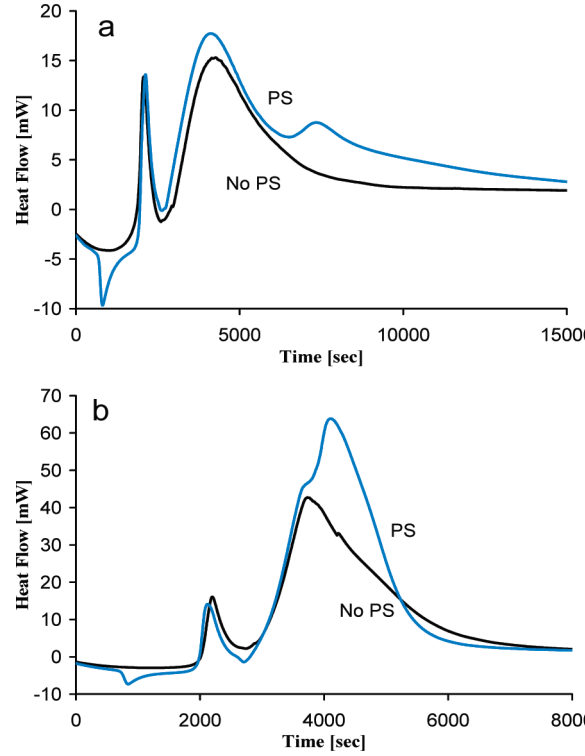

Figure 5. Differential scanning calorimetry analyses of the reactions of AB (150 mg) in bmimCl (150 mg) with 5.3 mol % PS (55 mg) at (a) 85 and (b) 110 °C. The initial exotherm is an apparatus artifact.

and 1.75 equiv, respectively, and at 6 h, 2.18 and 2.01 equiv. Thus, PS appears to have significantly enhanced the release rate of the second H_2 equivalent from AB. DSC measurements also support this conclusion. The black curve in Figure 5a shows a single, well-defined exotherm for the release of the first H_2 equivalent from the reaction of an AB/bmimCl mixture. The blue curve, which is from the reaction of a similar mixture containing 5.3 mol % of added PS, clearly exhibits a second exotherm, indicating the release of additional H_2 by a different process. Consistent with the H_2-release measurements that showed significant rate enhancements for the second H_2 equivalent as the temperature was raised, when the upper temperature of the DSC analysis was raised from 85 to 110 °C (Figure 5b), the second exotherm grew and shifted to shorter times such that it overlapped the first isotherm.

In order to better quantify the effects of both PS-loading and temperature, more detailed H_2-release data on a series of 50/50

Table 5. H_2-Release Data (Gas Buret) for AB/bmimCl/PS Reactions

temp (°C)	amount of PS (mol %, mg, mmol)	total wt (mg)[a]	time to H_2 equivalents (min) 0.75 equiv	1 equiv	1.5 equiv	final (equiv)
75		300	228	459		1041 (1.43)
	0.96, 10, 0.047	310	205	320	665	1040 (2)
	5.3, 55, 0.26	355	161	215	342	723 (1.99)
	24.9, 260, 1.21	560	140	208	378	782 (1.98)
85		300	52	84	199	316 (2)
	0.96, 10, 0.047	310	50	74	118	179 (2)
	5.3, 55, 0.26	355	45	61	95	171 (2)
	24.9, 260, 1.21	560	35	41	55	77 (2)
95		300	21	37	87	126 (2)
	0.96, 10, 0.047	310	20	27	44	72 (2)
	5.3, 55, 0.26	355	17	21	31	52 (2)
	24.9, 260, 1.21	560	16.3	20.9	32	59 (1.91)
110		300	5.8	7.4	12	20 (2)
	0.96, 10, 0.047	310	4.9	5.9	8	13 (2)
	5.3, 55, 0.26	355	3.8	4.3	6	9 (2)
	24.9, 260, 1.21	560	4.0	4.3	5	7 (2)

[a] 150 mg of NH_3BH_3 (4.87 mmol) and 150 mg of bmimCl were used for all reactions.

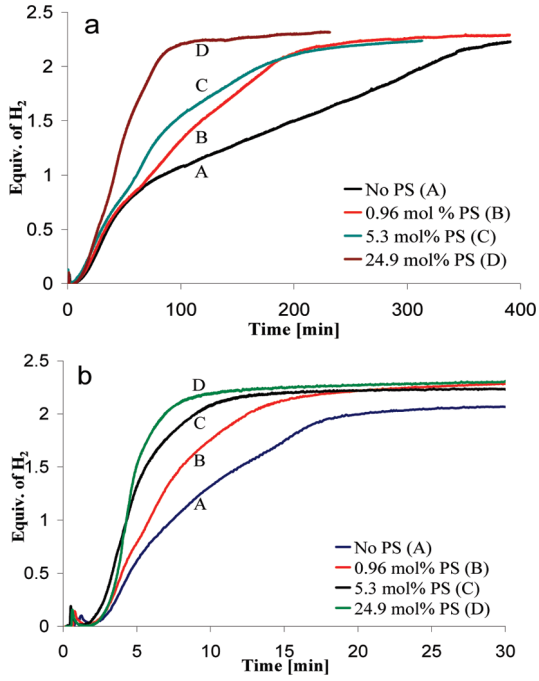

Figure 6. H_2-release measurements (gas buret) of the reaction of AB (150 mg) in bmimCl (150 mg) with 0, 0.96, 5.3, and 24.9 mol % PS (10, 55, and 260 mg) at (a) 85 and (b) 110 °C.

wt % AB/bmimCl systems containing from 0 to 24.9 mol % PS at 75, 85, 95, and 110 °C were collected on the automated gas buret (Table 5 and Figure 6). The rate of H_2-release increased as the mol % of PS in the mixture was increased. For example, as shown in Figure 6a, while the reaction at 85 °C without PS required 84 and 316 min to liberate the first and second equivalents of H_2, the reactions with 0.96 (first 74, second 179 min), 5.3 (first 61, second 171 min), and 24.9 (first 41, second 77 min) mol % PS were all significantly faster, with the fastest rate found for the highest loading. Substantial rate increases were observed for all reactions when the reaction temperature was increased. Thus, as illustrated in the plots in Figure 6b, at 110 °C the reaction without PS required only 7.4 and 20 min to liberate the first and second equivalents of H_2, but the reactions with 0.96 (first 5.9, second 13 min), 5.3 (first 4.3, second 9 min), and 24.9 (first 4.3, second 7 min) mol % PS were all again significantly faster. It is also noteworthy that at 95 and 110 °C, unlike at 85 °C, the rate of H_2-release for the 5.3 and 24.9 mol % PS reactions were similar, indicating that less PS is required to induce H_2-release at higher temperatures.

Table 6. H_2-Release (Toepler Pump) Data for Partially Dehydrogenated AB

time (h)	total wt (mg)[a]	H_2 released equiv	mmol
0	250	0.99	8.04
1[b]	500	1.05	8.51
2[b]	500	1.11	9.02
3[b]	500	1.27	10.30
21[b]	500	1.78	14.42
24[b]	500	1.79	14.51
0	250	0.98	7.96
1[c]	591	1.21	9.82
2[c]	591	1.45	11.75
3[c]	591	1.51	12.20
24[c]	591	1.70	13.77

[a] 250 mg of NH_3BH_3 (8.1 mmol) for all experiments. [b] 250 mg of bmimCl added after neat NH_3BH_3 reaction. [c] 250 mg of bmimCl and 91 mg of PS added after neat NH_3BH_3 reaction.

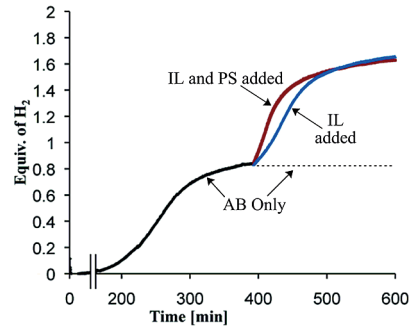

Figure 7. H_2-release measurements (gas buret) of partially dehydrogenated AB (150 mg) where 1 equiv of H_2 was initially released at 85 °C, and then bmimCl (150 mg) and bmimCl (150 mg)/PS (55 mg/5.2 mol %) were added to separate samples and heating resumed at 85 °C. the The dashed line shows the observed AB H_2-release when IL and/or PS are not added.

The above studies all indicate that both bmimCl and PS promote the loss of more than 1 equiv of H_2, with the combination of PS in bmimCl being the most effective. To further test this conclusion, two samples of neat AB were first heated at 85 °C for 23 h to produce a partially dehydrogenated material where only ~1.0 equiv of H_2 had been released. To the first sample was added bmimCl, and to the second sample were added both PS and bmimCl. The flasks were then reheated at 85 °C to produce liquid suspensions, and any additional H_2-release was measured. While the heating of AB in the solid state at 85 °C for more extended periods (~48 h) gave no further H_2-release, both Toepler-pump (Table 6) and gas-buret measurements (Figure 7) showed that the addition of either bmimCl or bmimCl/PS to the partially dehydrogenated AB caused H_2-release to resume, ultimately yielding an additional ~0.7 equiv of H_2 from both samples, with the bmimCl/PS reaction exhibiting the fastest rate.

While bmimCl is a liquid at 85 °C, it is a solid at room temperature; therefore, solid-state NMR was used to monitor the bmimCl/AB/PS reactions at different stages by heating the liquid mixtures at 85 °C and then quenching the reactions at the indicated times by cooling to room temperature, with subsequent analyses of the resulting solid materials by solid-

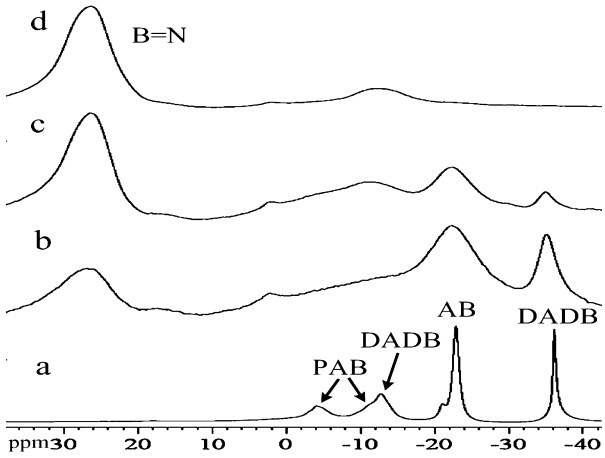

Figure 8. Solid-state ^{11}B NMR (240 MHz) spectra recorded at 25 °C of the reaction of AB (150 mg) and 5.3 mol % PS (55 mg) in bmimCl (150 mg) at 85 °C after the H_2-release of (a) 0.5 equiv (30 min), (b) 1 equiv (61 min), (c) 1.5 equiv (95 min), and (d) 2 equiv (171 min). The broad DADB resonance at −13 ppm is obscured by the AB and PAB resonances.

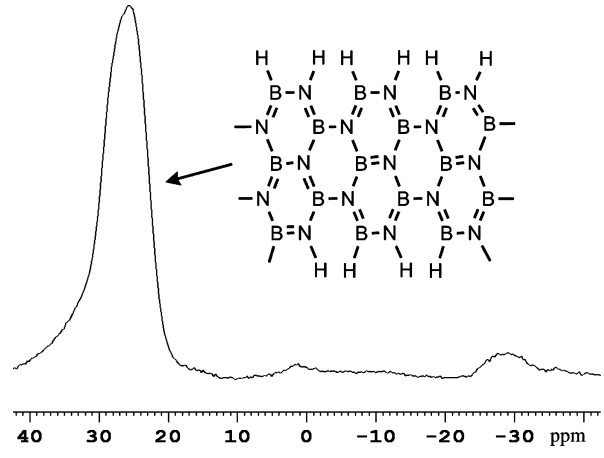

Figure 9. Solid-state ^{11}B NMR (240 MHz) spectrum recorded at 25 °C of the reaction of AB (250 mg) and 5.2 mol % PS (91 mg) in bmimCl (150 mg) at 85 °C for 23 h.

state ^{11}B NMR. Consistent with both the H_2-release measurements and the ^{11}B NMR studies of the solid-state PS/AB reactions, the solid-state ^{11}B spectrum (Figure 8) of the reaction of a 50/50 wt % bmimCl/AB mixture containing 5.2 mol % of added PS showed after 0.5 equiv of H_2-release the resonances of both DADB[37,38] and branched-chain PAB.[5] The small signal (−21.2 ppm) that is apparent just downfield of the AB (−23.2 ppm) resonance has a chemical shift value consistent with that previously reported[42−45] for the $H_3BNH_2^-$ anion (−21.49 ppm) and with its DFT/GIAO calculated value (−20.6 ppm) (Figure 2S, Supporting Information). As the reaction continued, the resonances broadened and diminished and a new resonance centered at 25.9 ppm grew in that is characteristic of unsaturated sp^2-hybridized boron. As shown in the spectrum in Figure 9, after prolonged reaction (23 h) only the 25.9 ppm resonance remained, indicating that all final products had unsaturated sp^2-hybridized structures. NMR studies of the dehydrogenated products of AB H_2-release promoted by solid-state thermal reactions[4] have likewise shown the formation of similar types of B═N unsaturated final products after more than 2 equiv of H_2-release.

In situ solution ^{11}B NMR studies of the PS-promoted H_2-release from AB in the room-temperature ionic-liquid mmimMeSO$_4$ at 85 °C also exhibited features similar to those observed in the solid-state NMR spectra of the bmimCl reactions. It is also significant that the ^{11}B NMR spectra of the reactions with and without PS in mmimMeSO$_4$ (Figure 10) showed the formation of similar types of products. In both reactions, DADB and PAB polymers were formed initially; at the longer times where more H_2 was released, the DADB and PAB resonances decreased and insoluble materials formed. Only a small intensity resonance was observed near 25 ppm, indicating that if unsaturated B═N products such as borazine or polyborazylene were formed, they must have reacted rapidly to form the final insoluble product.

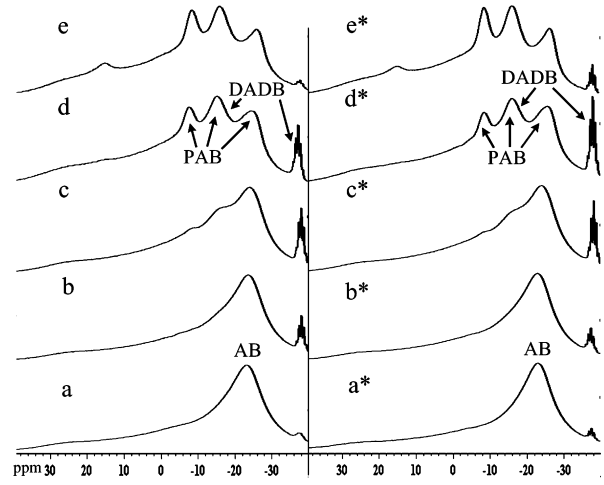

Figure 10. Solution ^{11}B NMR (128 MHz) spectra recorded at 25 °C of the reaction of AB (50 mg) in mmimMeSO$_4$ (450 mg) at 85 °C. (Right) With 5.2 mol % PS (18 mg) after the release of (a) 0.03, (b) 0.08, (c) 0.32, (d) 1.14, and (e) 1.63 equiv. (Left) Without PS after the release of (a*) 0.03, (b*) 0.08, (c*) 0.29, (d*) 1.07, and (e*) 1.62 equiv. The broad DADB resonance at −13 ppm is obscured by the AB and PAB resonances.

One of the barriers to the utilization of AB H_2-release for hydrogen storage is that AB dehydrogenation either in the solid state or in solution normally produces considerable foaming.[46] However, as shown in the photographs in Figure 11, Proton Sponge, besides increasing both the rate and extent of H_2-release, was found to have the unanticipated but highly beneficial effect of significantly reducing foaming during AB H_2-release in the bmimCl/PS reactions.

PS was also found to increase AB H_2-release in both other ionic liquids and tetraglyme, with both the extent and rate of H_2-release comparable to those of the PS/bmimCl reactions (Tables 7 and 8 and Figure 12). Gas-buret data at 85 °C for the tetraglyme reactions showed that fast rates could be achieved with only 1 mol % of PS. The ^{11}B NMR spectra of the tetraglyme/PS reactions also showed evidence for the initial formation of the $H_3BNH_2^-$ anion, followed by the appearance of the resonances for PAB polymers. However, at longer times, unlike in the ionic liquids, the major product was borazine (30.1

(42) Myers, A. G.; Yang, B. H.; David, K. J. *Tetrahedron Lett.* **1996**, *37*, 3623–3626.
(43) Kang, X.; Fang, Z.; Kong, L.; Cheng, H.; Yao, X.; Lu, G.; Wang, P. *Adv. Mater.* **2008**, *20*, 2756–2759.
(44) Xiong, Z.; Chua, Y. S.; Wu, G.; Xu, W.; Chen, P.; Shaw, W.; Karkamkar, A.; Linehan, J.; Smurthwaite, T.; Autrey, T. *Chem. Commun.* **2008**, 5595–5597.
(45) Xiong, Z.; Yong, C. K.; Wu, G.; Chen, P.; Shaw, W.; Karkamkar, A.; Autrey, T.; Jones, M. O.; Johnson, S. R.; Edwards, P. P.; David, W. I. F. *Nat. Mater.* **2008**, *7*, 138–141.
(46) Aardahl, C. L. DOE Hydrogen Program Review, 2008; http://www.hydrogen.energy.gov/pdfs/review08/st_5_aardahl.pdf.

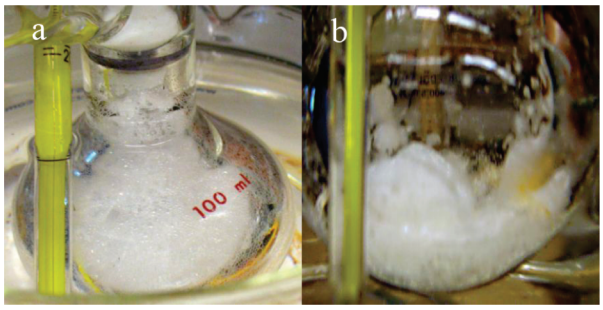

Figure 11. Foaming resulting from the reaction of 250 mg of AB in 250 mg of bmimCl after 1 h at 100 °C: (a) without PS and (b) with 5.2 mol % PS (91 mg).

Table 7. H_2-Release Data (Toepler Pump) for AB/Ionic-Liquid/PS Reactions at 85 °C

solvent	time (h)	amount of PS (mol %, mg, mmol)	total wt (mg)[a]	H_2 released equiv	H_2 released mmol
bdmimCl	1		500	0.68	5.52
	3		500	1.06	8.58
	6		500	1.31	10.61
	22		500	2.29	18.59
bdmimCl	1	5.2, 91, 0.43	591	1.26	10.19
	3	5.2, 91, 0.43	591	1.82	14.74
	6	5.2, 91, 0.43	591	2.03	16.47
	22	5.2, 91, 0.43	591	2.13	17.23
$edmimEtSO_4$	1		500	1.00	8.09
	3		500	1.32	10.7
	6		500	1.64	11.3
	22		500	2.20	17.8
$edmimEtSO_4$	1	5.2, 91, 0.43	591	1.52	12.33
	3	5.2, 91, 0.43	591	1.91	15.50
	6	5.2, 91, 0.43	591	2.04	16.51
	21.5	5.2, 91, 0.43	591	2.16	17.47
tetraglyme	1		500	1.19	9.65
	3		500	1.80	14.57
	6		500	1.97	15.97
	22		500	2.12	17.20
tetraglyme	1	5.2, 91, 0.43	591	1.32	10.73
	3	5.2, 91, 0.43	591	1.66	13.45
	6	5.2, 91, 0.43	591	1.86	15.10
	22	5.2, 91, 0.43	591	2.13	17.22

[a] 250 mg of NH_3BH_3 (8.1 mmol) and 250 mg of ionic liquid or tetraglyme were used for all reactions.

ppm)[47] along with smaller amounts of BH_4^- (−36.8 ppm)[47] and μ-aminodiborane (−27.5 ppm)[47] (Figure 13). Thus, ionic-liquid solvents are favored for AB H_2-release since they suppress or reduce the formation of these products.

We have previously proposed[5] that the AB activation for H_2-release that is observed in ionic liquids may occur by a mechanistic pathway involving (1) ionic-liquid-promoted conversion of AB into its more reactive ionic DADB form, (2) further intermolecular dehydrocoupling reactions between hydridic B−H hydrogens and protonic N−H hydrogens on DADB and/or AB to form neutral PAB polymers, and (3) PAB dehydrogenation to unsaturated cross-linked polyborazylene materials. The initial formation of DADB has also been

(47) Nöth, H.; Wrackmeyer, B. *Nuclear Magnetic Resonance Spectroscopy of Boron Compounds*; Springer-Verlag: New York, 1978; pp 188, 265, 394−395.

Table 8. H_2-Release Data (Gas Buret) for AB/Tetraglyme/PS Reactions at 85 °C

amount of PS (mol %, mg, mmol)	total wt (mg)[a]	time to H_2 equivalents (min) 1 equiv	1.5 equiv	final (equiv)
	300	248	587	1126 (2)
0.96, 10, 0.047	310	166	234	461 (2)
5.3, 55, 0.26	355	164	263	886 (2)
24.9, 260, 1.21	560	193	458	1238 (1.91)
	300	40.7	80.4	211 (2)
0.96, 10, 0.047	310	36.1	51.4	125 (2)
5.3, 55, 0.26	355	27.8	51.6	253 (1.87)
24.9, 260, 1.21	560	34.9	107	325 (1.76)
	300	17.2	39.6	122 (2)
0.96, 10, 0.047	310	14.4	22.9	77.1 (2)
5.3, 55, 0.26	355	12.1	25.2	169 (2)
24.9, 260, 1.21	560	18.5	87.2	369 (1.88)

[a] 150 mg of NH_3BH_3 (4.87 mmol) and 150 mg of tetraglyme were used for all reactions.

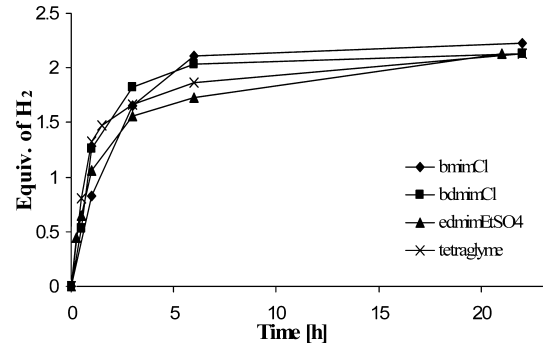

Figure 12. H_2-release measurements (Toepler pump) of the reaction of AB (250 mg) in ionic liquids or tetraglyme (250 mg) with 5.2 mol % PS (91 mg) at 85 °C.

proposed as a key step in thermally induced AB H_2-release reactions in the solid state and in organic solvents.[4,48] While a DADB pathway may contribute to the H_2-release observed in the bmimCl/PS solutions, their observed rate enhancements and DSC properties suggest that there is also another mechanistic pathway for H_2-release in these systems.

Proton Sponge is a strong base and because of its low nucleophilicity is frequently used as a deprotonating agent in organic and inorganic syntheses that can eliminate the undesirable side reactions often found with more coordinating bases.[30] The observation of a signal near −21.0 ppm in the ^{11}B NMR spectra at the beginning stages of the reactions of AB with PS in both ionic liquids and tetraglyme strongly supports a PS-promoted AB H_2-release reaction pathway involving initial AB deprotonation to form the $H_3BNH_2^-PSH^+$ ion.

Deprotonation of AB by bases is well-known. For example, the $H_3BNH_2^-Li^+$ salt has previously been prepared *in situ* from AB and *n*-BuLi at 0 °C.[42] More recently, ball milling[43,45,49] and solution[50,51] reactions of AB with metal hydrides have been used to generate $H_3BNH_2^-M^+$ (M = Li and Na) and $(H_3BNH_2^-)_2Ca^{2+}$. We found that AB deprotonation could also be easily achieved by its reaction with either lithium or potassium triethylborohydride (eq 7), but in these cases a Et_3B-

(48) (a) Shaw, W. J.; Linehan, J. C.; Szymczak, N. K.; Heldebrant, D. J.; Yonker, C.; Camaioni, D. M.; Baker, R. T.; Autrey, T. *Angew. Chem., Int. Ed.* **2008**, *47*, 7493–7496. (b) Heldebrant, D. J.; Karkamkar, A.; Hess, N. J.; Bowden, M.; Rassat, S.; Zheng, F.; Rappe, K.; Autrey, T. *Chem. Mater.* **2008**, *20*, 5332–5336.

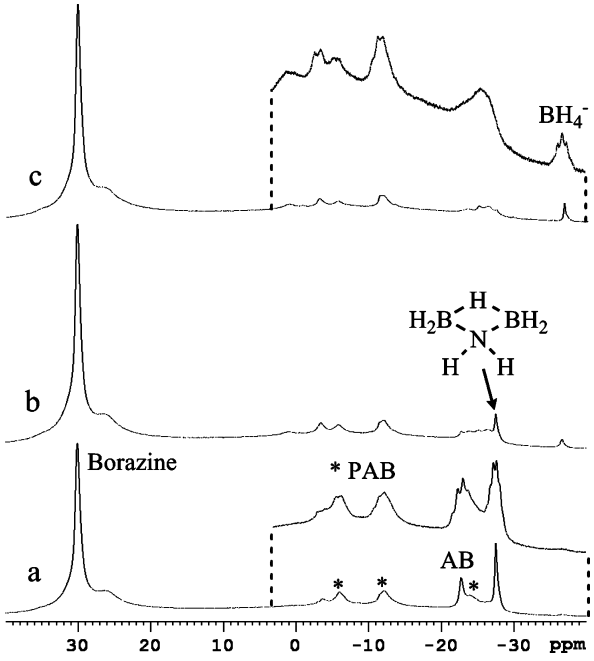

Figure 13. Solution $^{11}B\{^1H\}$ NMR (128 MHz) spectra (insets show ^1H-coupled spectra) recorded at 80 °C of the reaction of AB (50 mg) and 5.2 mol % PS (18 mg) in tetraglyme (450 mg) at 85 °C after (a) 1, (b) 3, and (c) 6 h.

stabilized anion was formed, with the observed resonances in the ^{11}B NMR spectra of the Li^+ (−7.5 (s) and −23.8 (q) ppm) and K^+ (−7.8 (s) and −23.6 (q) ppm) compounds being assigned on the basis of the DFT/GIAO calculations to the BEt_3− (calcd −10.6) and terminal $-BH_3$ (calcd −25.3) units in the anion.

$$H_3BNH_3 + M^+BEt_3H^- \rightarrow [Et_3BNH_2BH_3]^-M^+ + H_2 \quad (M = Li \text{ or } K) \quad (7)$$

The structures of $H_3BNH_2^-M^+$ (M = Li and Na) and $(H_3BNH_2^-)_2Ca^{2+}$ have recently been established from the analyses of their high-resolution powder diffraction data,[49,51] and the structure of $(H_3BNH_2^-)_2Ca^{2+}\cdot 2THF$ has been established by a single-crystal X-ray determination.[50] Our crystallographic determination of the $[Et_3BNH_2BH_3]^-K^+\cdot$18-crown-6 complex in Figure 14 confirmed that, following AB nitrogen-deprotonation by the triethylborohydride, the Lewis-acidic triethylborane group coordinated at the nitrogen. Selected bond lengths and angles are listed in the figure caption. The angles around B1 indicate sp^3 hybridization resulting from the nitrogen lone-pair donation to the vacant boron orbital on the triethylborane fragment. The observed N2−B3 length of 1.594(2) Å is similar to that found in AB (1.58(2) Å)[52] but longer than those determined in the powder diffraction studies of $H_3BNH_2^-Li^+$ (1.561(7) Å) and $(H_3BNH_2^-)_2Ca^{2+}$ (1.575(4) Å).[51] The longer distance of the B1−N2 1.631 (2) Å bond compared to that of N2−B3 is consistent with the higher Lewis acidity of the H_3B fragment (and hence stronger N→B dative bonding donation) compared to the Et_3B unit. The K^+ cation is coordinated to the six oxygen atoms of the 18-crown-6 ring with distances ranging from 2.79 to 2.92 Å. Consistent with the hydridic nature of the BH hydrogens of $Et_3BNH_2BH_3^-$, the closest interactions of the

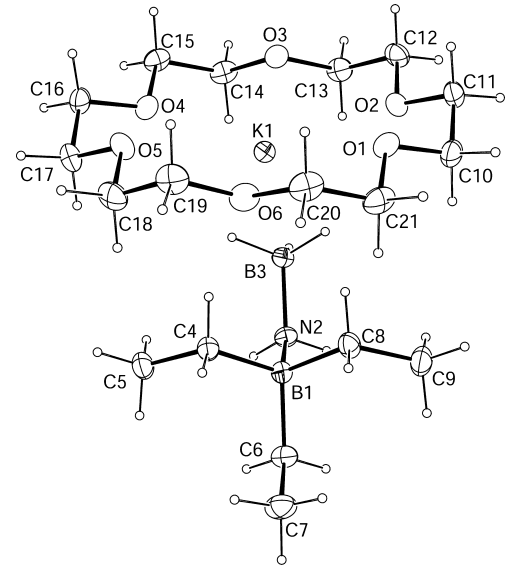

Figure 14. Selected bond distances (Å) and angles (°) for $[Et_3BNH_2BH_3]^-K^+\cdot$18-crown-6: B3−N2, 1.594(2); B1−N2, 1.630(2); B1−C4, 1.622(2); B1−C6, 1.637(2); B1−C8, 1.629(2); B3−H3a, 1.13(2); B3−H3b, 1.14(2); B3−H3c, 1.13(2); N2−H2a, 0.94(2); N2−H2b, 0.91(2); K1−H3a, 2.85(2); K1−H3c, 2.76(2); B1−N2−B3, 122.05(10); N2−B1−C4, 108.75(11); N2−B1−C6, 105.17(10); N2−B1−C8, 108.43(11); B1−N2−H2a, 107.0(11); B1−N2−H2b, 107.6(10); H2a−N2−H2b, 106(2).

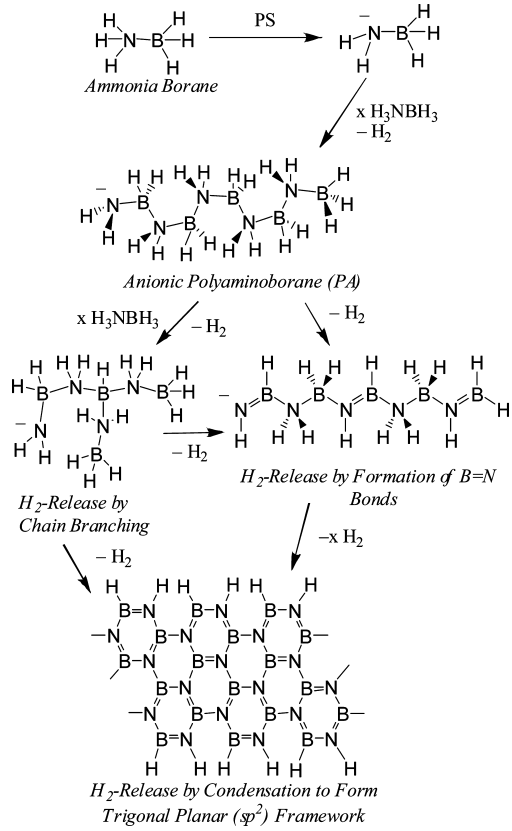

Figure 15. Possible anionic polymerization pathway for PS-promoted H_2-release from AB.

(49) Ramzan, M.; Silvearv, F.; Blomqvist, A.; Scheicher, R. H.; Lebegue, S.; Ahuja, R. *Phys. Rev. B: Condens. Matter Mater. Phys.* **2009**, *79*, 132102-4.
(50) Diyabalanage, H. V. K.; Shrestha, R. P.; Semelsberger, T. A.; Scott, B. L.; Bowden, M. E.; Davis, B. L.; Burrell, A. K. *Angew. Chem., Int. Ed.* **2007**, *46*, 8995–8997.
(51) Wu, H.; Zhou, W.; Yildirim, T. *J. Am. Chem. Soc.* **2008**, *130*, 14834–14839.
(52) Klooster, W. T.; Koetzle, T. F.; Siegbahn, P. E. M.; Richardson, T. B.; Crabtree, R. H. *J. Am. Chem. Soc.* **1999**, *121*, 6337–5343.

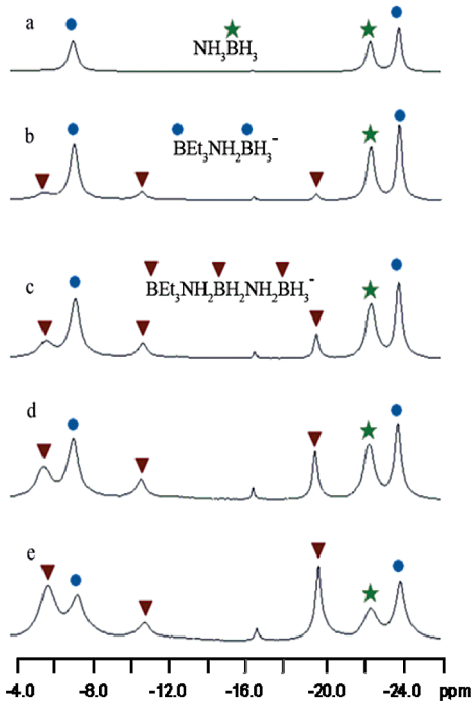

Figure 16. Reaction progression monitored by $^{11}B\{^1H\}$ NMR of the reaction of $[Et_3BNH_2BH_3]^-Li^+$ and AB at room temperature, showing the growth of the $[Et_3BNH_2BH_2NH_2BH_3]^-$ resonances: (a) 0, (b) 18, (c) 44, (d) 67, and (e) 144 h.

K^+ to the $Et_3BNH_2BH_3^-$ anion are with two of the BH hydrogens, K1−H3a 2.85(2) Å and K1−H3c 2.76(2) Å.

Electronic structure calculations on $[H_2NBH_3]^-M^+$ have predicted[49,51] that the B−H hydrogens in these complexes will be much more negatively charged and, as a result, have a higher basicity than in AB. This increases the ability of these anions to release H_2 by the intermolecular reaction of their hydridic B−H hydrogens with an N−H proton on an adjacent complex. Thus, the most likely second step in PS-promoted AB H_2-release is the intermolecular dehydrocoupling of one of the hydridic B−H hydrogens of $[H_2NBH_3]^-PSH^+$ with a H_3NBH_3 to produce, as shown in Figure 15a, a growing anionic PAB polymer. DFT/GIAO calculations of model anionic polymers showed that their ^{11}B NMR chemical shifts (Figure 2S, Supporting Information) would be indistinguishable from those of the corresponding neutral PAB polymers,[5] thus explaining the similarity of the spectra for the reactions with and without PS in Figure 10.

The expected decreased acidity of the internal NH_2 hydrogens of a PAB polymer relative to those on terminal NH_3 units should result in the NH_2 protons being less reactive for dehydrocoupling reactions that could liberate more than 1 equiv of H_2. Thus, the increased release rate for the second equivalent of H_2 observed for the PS-induced reactions of AB may result from the greater ability of the more basic B−H hydrogens of an *anionic* PAB to induce H_2-elimination reactions with the protons at these NH_2 sites.

As a model for the anionic polymerization step, we explored the reactions of $[Et_3BNH_2BH_3]^-Li^+$ with AB. The higher Lewis acidity of the BH_3 group compared to the Et_3B unit should significantly increase the nucleophilic character of the boron−hydrogens and enhance the ability of this anion to undergo dehydropolymerization with AB. In agreement with this expectation, Toepler-pump measurements confirmed the loss of H_2 during the reaction of equal equivalents of NH_3BH_3 with $[Et_3BNH_2BH_3]^-Li^+$ at 23 °C, and an electrospray mass spectrum

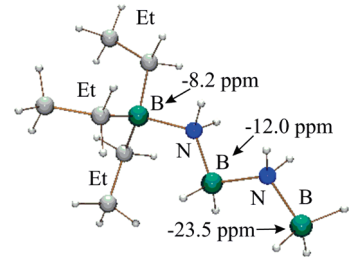

Figure 17. DFT (B3LYP/6-31G(d))-optimized geometry and GIAO (B3LYP/6-311G(d)) calculated ^{11}B NMR shifts for $[Et_3BNH_2BH_2NH_2BH_3]^-$.

indicated formation of $Et_3BNH_2BH_2NH_2BH_3^-$ (eq 8). As shown in the ^{11}B NMR spectra in Figure 16, new resonances grew in at −6.0 (s, Et_3B−), −10.9 (t, $-NH_2BH_2-$), and −19.6 (q, $-BH_3$) that are in good agreement with the calculated ^{11}B NMR shifts for the DFT-optimized geometry of the chain growth product $Et_3BNH_2BH_2NH_2BH_3^-$ given in Figure 17.

$$[Et_3BNH_2BH_3]^-Li^+ + H_3BNH_3 \rightarrow [Et_3BNH_2BH_2NH_2BH_3]^-Li^+ + H_2 \quad (8)$$

When the reaction was carried out at higher temperatures, the growth of the BNH_x oligomers $Et_3B(NH_2BH_2)_2NH_2BH_3^-$ and $Et_3B(NH_2BH_2)_3NH_2BH_3^-$ was observed in the electrospray mass spectra. These results provide additional strong support for a PS-induced H_2-release mechanism involving an intermolecular anionic dehydropolymerization pathway initiated by the $NH_2BH_3^-$ anion.

In summary, base-activation by Proton Sponge of AB H_2-release has been demonstrated in solid-state and in ionic-liquid and tetraglyme solution reactions, with the experimental observations and model studies supporting an anionic dehydropolymerization mechanism initiated by the $H_3BNH_2^-$ anion. For the bmimCl/PS reactions, significantly increased rates of AB H_2-release, yielding over 2 equiv of H_2, were achieved with as little as 1 mol % Proton Sponge. These studies also further demonstrate that H_2-release from chemical hydrides can occur by a number of different mechanistic pathways and strongly suggest that optimal chemical-hydride-based H_2-release systems may require the use of synergistic dehydrogenation methods to induce H_2-loss from chemically different intermediates formed during release reactions.

Acknowledgment. We thank the U.S. Department of Energy for grants from the Center of Excellence for Chemical Hydrogen Storage and the Division of Basic Energy Sciences for the support of this research. A portion of the research was performed in the Environmental Molecular Sciences Laboratory, a national scientific user facility sponsored by the Department of Energy's Office of Biological and Environmental Research, located at Pacific Northwest National Laboratory. We especially thank Dr. Tom Autrey for his generous invitation to visit PNNL, Dr. Wendy Shaw and Dr. Sarah Burton for their assistance with the solid-state NMR, and Dr. Ahbi Karkamkar for assistance with the DSC used in this study.

Supporting Information Available: Diagram of the Toepler pump apparatus used for some H_2-release measurements; tables listing the Cartesian coordinates for all DFT-optimized geometries; X-ray crystallographic data for the structure determination of $[Et_3BNH_2BH_3]^-K^+ \cdot$18-crown-6 (CIF); complete ref 36. This material is available free of charge via the Internet at http://pubs.acs.org.

JA905015X